Heme Binding by the N-Terminal Fragment 1−44 of Human Growth Hormone†

Barbara Spolaore, Vincenzo De Filippis, and Angelo Fontana*

CRIBI Biotechnology Centre, University of Padua, Viale G. Colombo 3, 35121 Padua, Italy

Received July 15, 2005; Revised Manuscript Received September 26, 2005

ABSTRACT: Fragment 1−44 of human growth hormone (hGH), prepared in vitro by limited proteolysis of the hormone with pepsin at low pH, encompasses in full the N-terminal helix of this four-helix bundle protein [Spolaore, B., Polverino de Laureto, P., Zambonin, M., and Fontana, A. (2004) *Biochemistry 40*, 9460−9468]. Here, we report the new and interesting observation that fragment 1−44 can bind heme. The binding property is specific for the N-terminal helix of hGH, since heme binding does not occur with fragment 45−191 or the entire protein. The spectral characteristics of Fe-protoporphyrin IX are those of a low-spin, hexacoordinated iron ligated by two imidazole rings of His residues or His and Met residues. Far-UV circular dichroism (CD) measurements revealed that fragment 1−44 acquires a helical secondary structure upon heme binding. Heme appears to be bound to the fragment in a stereospecific way, since an induced dichroic signal is observed in the Soret region of the CD spectrum. The heme−fragment complex occurs in a 1:1 molar ratio, as determined by spectrophotometric titration, as well as by electrospray-ionization mass spectrometric analysis of the complex. The fragment alone is much more susceptible to tryptic digestion than the heme complex, implying a more folded and rigid structure of this last species. It is proposed that the molecular features of fragment 1−44 determining its heme-binding property reside in the amphipathic character of the helix adopted by the fragment, as well as in the presence in its polypeptide chain of His18, His21, and Met14. These residues can act as specific ligands for the heme-iron, as observed with cytochromes.

Heme (Fe-protoporphyrin IX) is a protein cofactor that nature uses frequently to achieve different important functions, such as reversible O_2 binding, O_2 activation, decomposition of peroxides, and electron transfer (*1*). Moreover, it has been shown that heme can regulate many biological processes, including transcription, translation, protein translocation, and erythroid differentiation (*2*). Most of the natural heme-binding proteins fold into α-helical structures and upon removal of heme adopt a partly folded (*3*−*6*) or largely unfolded (*7, 8*) state. The family of heme proteins has been extensively studied, mostly with the aim to unravel the protein structural features which are important for an efficient binding of heme and related biological functions. Indeed, heme binding imposes strong constraints to the structure of a protein, which can be stronger than those caused by the packing of a hydrophobic core (*9*). The major contribution to the affinity of heme is due to a nonspecific partitioning of heme into a hydrophobic region of a protein, which accounts for the tendency of heme to adsorb to a variety of proteins (*10*−*15*). Second, a specific binding of the heme is dictated by the formation of coordination bonds with the imidazole ring of histidine and/or other specific interactions with amino acid residues surrounding the porphyrin ring (*16, 17*). Heme protein design is also nowadays intensively pursued with the goal to better understand structure−function relationships in heme proteins and to design molecules with new desired functions (*17*−*21*). Protein helical scaffolds have been mostly used by protein designers, due to the prevalence of α-helical heme proteins in nature and the relatively easy de novo design of helical polypeptides (*22*−*28*). However, heme affinity measurements have demonstrated that even the best designed protein moieties bind heme much more weakly than natural heme proteins (*17, 21*).

Human growth hormone (hGH[1]) is a four-helix bundle protein of 191 amino acid residues (*29*) that principally regulates the body growth, but affects also the metabolism of proteins, carbohydrate, and lipids (*30*−*32*). A proposal was advanced that hGH acts also as a pro-hormone and, therefore, that it requires its proteolytic cleavage to produce various peptide fragments that display the diversity of biological effects of hGH (*33*). It has been reported that two fragments of hGH are present in vivo: fragment 1−43, which shows insulin-potentiating effects, and fragment 44−191, which has diabetogenic activity (*34*−*36*). These fragments have been detected in serum and at the level of the pituitary gland (*34, 37, 38*), but their mechanisms of formation from the parent protein are not known. Since they are two complementary parts of the 191-residue chain of hGH, it is

† This work was supported in part by the Italian Ministry of University and Research (FIRB Project on Protein Folding and PRIN-2003).

* To whom correspondence should be addressed. Tel.: +39-049-8276156. Fax: +39-049-8276159. E-mail: angelo.fontana@unipd.it.

[1] Abbreviations: hGH, human growth hormone; CD, circular dichroism; ESI, electrospray ionization; E/S, enzyme-to-substrate ratio; ESI, electrospray-ionization; Gdn·HCl, guanidine hydrochloride; HPLC, high performance liquid chromatography; kDa, kilodalton; RP, reverse-phase; MS, mass spectrometry; TFA, trifluoroacetic acid; Tris, tris(hydroxymethyl)aminomethane; UV, ultraviolet; 1−44, N-terminal fragment of hGH.; 45−191, C-terminal fragment of hGH cross-linked by two disulfide bridges (Cys53−Cys165 and Cys182−Cys189); RR, resonance Raman.

10.1021/bi051374d CCC: $30.25
Published on Web 11/16/2005

conceivable to suggest that they are formed by selective proteolytic cleavage of the native protein. However, at present the specific protease responsible for their generation has not been identified.

In a recent paper, we have shown that limited proteolysis of hGH in vitro by pepsin at pH 4.0 leads to the production of fragments 1−44 and 45−191, as a result of the selective cleavage of the Phe44−Leu45 peptide bond (*39*). Therefore, the two peptic fragments of hGH prepared in vitro are related to the two physiologically relevant fragments occurring in vivo. It has been found that fragment 45−191, encompassing helixes 2, 3, and 4 of hGH and containing the two disulfide bridges of the protein (*29*), adopts a helical conformation in solution at neutral pH. Conversely, fragment 1−44, comprising the first helix of the native hormone, is rather disordered. Here, we report that the hGH fragment 1−44 of hGH can bind heme with high specificity. This binding phenomenon has been discovered by serendipity. Indeed, during a purification step of the fragment by size-exclusion chromatography, we have found that it was eluted complexed to heme from a gel filtration column that had been inadvertently polluted by heme in previous separations of myoglobin using the same column. Upon binding of the heme moiety, the fragment acquires a helical secondary structure, as judged from far-UV circular dichrosim (CD) measurements. The conformational properties of the heme−fragment complex, as well as the spectroscopic features of the heme when bound to the fragment, have been investigated. The molecular features of the hGH fragment 1−44 that likely dictate its heme-binding properties are discussed.

MATERIALS AND METHODS

Materials. Recombinant human growth hormone (hGH) was produced in *Bacillus subtilis* (*40*) and stored as a lyophilized sample at 4 °C. The protein was shown to be homogeneous by reverse-phase high-performance liquid chromatography (RP-HPLC) and by sodium dodecyl sulfate (SDS) polyacrylamide gel electrophoresis (PAGE) and to possess the correct N-terminal sequence. Pepsin, trypsin, hemin, and sodium dithionite were obtained from Sigma. Acetonitrile and trifluoroacetic acid (TFA) were purchased from Fluka. All other chemicals were analytical grade and were obtained from Sigma or Fluka. Water used to prepare buffers was purified by a Millipore Milli-Q Plus system.

Preparation of Fragment 1−44 and Fragment 45−191. Fragments 1−44 and 45−191 were produced by limited proteolysis of hGH at pH 4.0 following essentially the procedure described previously (*39*). Briefly, the reaction was performed on a solution of hGH (0.25 mg/mL) in 10 mM Na citrate/0.15 M NaCl, pH 4.0, at 4 °C with a protease:substrate (E:S) ratio of 1:10 (by mass) for 2 h and then stopped by alkalinization of the reaction mixture with 5% aqueous ammonia. Purification of fragments 1−44 and 45−191 from the limited proteolysis reaction mixture was performed by RP-HPLC utilizing a Vydac C_{18} column (10 × 250 mm) purchased from The Separations Group (Hesperia, CA). The column was eluted at a flow rate of 2.5 mL/min with a linear gradient of water and acetonitrile containing 0.1% and 0.085% TFA respectively, from 30% of acetonitrile to 55% in 8 min and from 55% to 63% in 26 min. The effluent from the column was monitored by measuring the absorbance at 226 nm.

All experiments were performed on fragment 1−44 and fragment 45−191 recovered after gel filtration chromatography. To this aim, both hGH fragments purified by RP-HPLC were lyophilized using the Speed-Vac system (Savant), redissolved in 6 M Gdn·HCl and loaded (250 μL, ∼1 mg/mL) on a Superdex-75 column (type HR 10/30, 1 × 30 cm; Pharmacia) equilibrated and eluted with 20 mM Tris·HCl/0.15 M NaCl, pH 7.5, at a flow rate of 0.4 mL/min. The absorbance of the effluent was recorded at 226 nm. The column was calibrated using a protein mixture kit of low molecular mass for gel filtration chromatography (Pharmacia).

UV−Visible Absorption Spectroscopy. Protein and heme concentrations were determined using a Perkin-Elmer Lambda-25 spectrophotometer. The concentrations of hGH and fragments 1−44 and 45−191 were determined from absorbance measurements at 280 nm according to Gill and von Hippel (*41*). Stock heme solutions were prepared in 0.1 M NaOH, and the precise concentration of heme was determined using an extinction coefficient for heme of 5.84×10^4 cm^{-1} M^{-1} at 385 nm (*42*). Heme stock solutions were then prepared in 20 mM Tris·HCl/0.15 M NaCl, pH 7.5, immediately before use. Reduction of the heme bound to fragment 1−44 was conducted by adding to the solution of the heme−fragment complex a 1000-fold molar excess of sodium dithionite, taken from a freshly prepared stock solution of the reagent.

Spectrophotometric titration of the binding of heme to fragment 1−44 was performed as described by Tsutsui and Mueller (*43*). A heme stock solution was added simultaneously into two cuvettes, one containing a solution 5.3 μM fragment 1−44 in 0.1 M Tris·HCl/0.15 M NaCl buffer, pH 7.5, and the other containing buffer only (reference cuvette). The stock solution (0.58 mM) of heme in 0.1 M NaOH was added at increments of 5, 10, 20, and 25 μL. After each addition of heme, the samples in the two cuvettes were stirred for 5 min and allowed to stand for an additional 5 min. Then, difference absorption spectra were recorded. These spectra had a maximum at 414 nm and a minimum at 368 nm. The heme-binding curve was constructed by plotting the $\Delta A_{414\ nm}$ versus the heme concentration. The titration of fragment 1−44 with heme was followed also by acquiring far-UV circular dichroism (CD) spectra of the fragment solution after successive additions of aliquots of a stock solution of heme. A titration curve was derived by plotting heme concentrations versus the variation of the mean residue ellipticity at 222 nm. The two heme-binding curves obtained by UV and far-UV CD measurements were fitted to the equation for the dissociation constant K_d assuming a 1:1 binding (*44*, *45*). For the curve fitting the Microcal Origin software (Microcal Software Inc., USA) was used.

Circular Dichroism. CD measurements were made at 25 °C on a Jasco J-710 spectropolarimeter (Tokyo, Japan) equipped with a thermostatically controlled cell holder. The instrument was calibrated with *d*-(+)10-camphorsulfonic acid. Far-UV CD spectra were recorded at a fragment concentration of 0.028 mg/mL using a quartz cell with a path length of 1 cm, and the results were expressed as mean residue ellipticity [θ] (deg·cm^2·$dmol^{-1}$). Far-UV CD spectra were analyzed in order to estimate the percentage of protein secondary structure using the equation reported by Scholtz et al. (*46*). The CD measurements in the 350−500 nm region

were obtained with a solution of fragment 1−44 (19.2 μM) containing heme (38 μM) using a quartz cell of 1.0 cm path length. The ellipticity (θ_{obs}) was expressed in millidegrees.

Resonance Raman Spectroscopy. Resonance Raman (RR) spectra of the heme−fragment complex were recorded at room temperature in 20 mM Tris·HCl/0.15 M NaCl buffer, pH 7.5, following essentially procedures before described (*47*).

Electrospray Mass Spectrometry. Mass spectra were acquired on a tandem mass spectrometer Q-TOF Micro (Micromass, U.K.) equipped with a Z-spray nanoflow electrospray-ionization (ESI) interface. Mass spectra (positive ion mode) of tryptic peptides of fragment 1−44 were acquired using the electrospray source operating at capillary, cone, and extractor voltages of 3200, 45, and 1 V, respectively. The temperature of the source was 80 °C and that of the desolvation gas 250 °C. For the MS analysis, samples were dissolved in a 1:1 solution of acetonitrile:water containing 1% formic acid.

The heme−fragment complex was analyzed by nano-electrospray mass spectrometry (MS). Nano-ESI capillaries were prepared in house from borosilicate glass tubes of 1 mm OD and 0.78 mm ID (Harvard Apparatus, Holliston, MA) using a micropipet puller (Sutter Instruments, Hercules, CA, model P-80 PC) and gold coated using an Edwards S-150B sputter coater (Edwards High Vacuum, West Sussex, U.K.). Typically, 0.5−2 μL of solution were analyzed. For the MS analysis the following experimental parameters were used (positive ion mode): capillary voltage, 1.7 kV; sample cone, 30.0 V; extractor cone, 1.0 V. In the collision cell argon was at an inlet pressure of 10 psi and the collision energy setting was 4.0 V. The ESI source temperature was set at 30 °C.

MS/MS analyses of the heme−fragment complex were performed utilizing the same parameters of the MS instrument as above. The collision gas was argon at an inlet pressure of 10 psi, and the collision energy setting was 45 V. Instrument control and data acquisition and processing were achieved using the MassLynx software (Micromass, U.K.).

MS analyses on fragment 1−44 were made utilizing a fragment sample which was recovered after gel filtration chromatography using a Superdex-75 column equilibrated and eluted with 0.1 M ammonium acetate, pH 7.5. Samples of fragment 1−44 in acetate buffer (10.6 μM) were mixed with aliquots of a freshly prepared solution of heme in 0.01 M NaOH (88 μM). Mass spectra of all fragment samples were acquired after 30 min incubation at room temperature.

Limited Proteolysis Experiments. Fragment 1−44 in the presence or absence of heme was subjected to limited proteolysis with trypsin. The reactions were performed in parallel on two solutions of fragment 1−44 (0.07 mg/mL) in 20 mM Tris·HCl/0.15 M NaCl, pH 7.5, one in the presence of heme at a molar ratio 1:3 of fragment over heme and the other in the absence of heme. After 30 min incubation, trypsin was added to both solutions at a protease:substrate (E:S) ratio of 1:500 (by weight). Aliquots were taken from the two reaction mixtures at intervals, and then proteolysis was quenched by acidification with an aqueous solution of 5% TFA. Samples were loaded onto a Zorbax Eclipse XDB-C_8 column (4.6 × 150 mm; Agilent Technologies, Palo Alto, CA) equilibrated with a mixture of 20% acetonitrile in water containing 0.085% TFA and eluted with a linear gradient of acetonitrile from 20% to 52% in 22 min at a flow rate of 0.8 mL/min. The absorbance of the effluent was recorded at 226 nm. The percent recoveries during proteolysis of fragment 1−44 and fragment 1−38 (which is formed in trace amounts and elutes at the same retention time of the intact fragment) and fragment 1−41 were determined by integrating the area under the HPLC peak of each fragment.

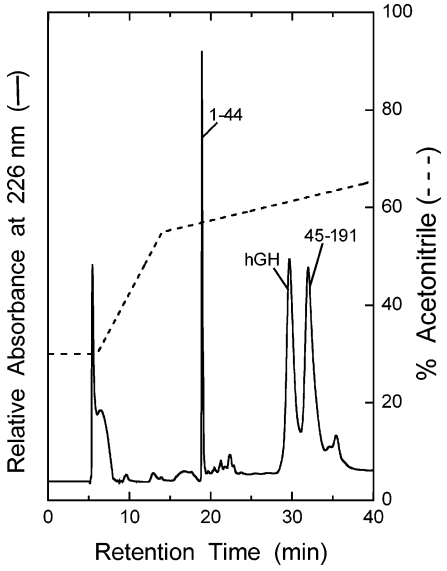

FIGURE 1: RP-HPLC analysis of the proteolytic mixture of hGH with pepsin. Proteolysis was conducted for 2 h at 4 °C (E/S 1/10, by weight) in 10 mM Na citrate/0.15 M NaCl buffer, pH 4.0. The chromatographic peaks containing hGH and fragments 1−44 and 45−191 are indicated in the chromatogram. A Vydac C_{18} column (10 × 250 mm) was employed as described under Materials and Methods.

RESULTS

Limited proteolysis of hGH with pepsin in 10 mM Na citrate/0.15 M NaCl, pH 4.0, at 4 °C occurs selectively at the level of the peptide bond Phe44−Leu45 (*39*). The reaction is quite clean, and it allows the selective production of fragment 1−44 and fragment 45−191, as shown by the RP-HPLC chromatogram of an aliquot of the reaction mixture (Figure 1). It was convenient to stop the proteolysis reaction after 2 h, in order to minimize the subsequent proteolytic degradation of the two fragments, especially fragment 1−44. Both fragments were purified first by RP-HPLC and then by gel filtration chromatography utilizing a Superdex-75 column equilibrated and eluted with 20 mM Tris·HCl/0.15 M NaCl buffer, pH 7.5 (not shown). The gel filtration step was used for separating the fragments from some aggregated material, as well as for preparing suitable solutions of homogeneous fragments for subsequent studies. The homogeneity of the fragments thus produced was established by a variety of analytical criteria, including electrospray-ionization (ESI) mass spectrometry (MS) (see also ref *39*).

The first indication that the hGH fragment 1−44 was able to bind heme was derived from the fact that the fragment solution prepared after gel filtration was reddish. Then, it was realized that the colored solution was due to the fact that the Superdex-75 column was earlier used by us with samples of the heme-containing protein myoglobin. The

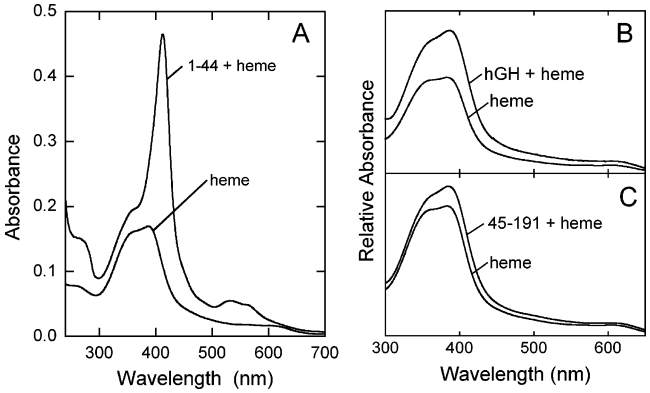

FIGURE 2: Absorption spectra of heme in the absence and presence of fragment 1−44 (A), hGH (B), and fragment 45−191 (C). (A) UV−vis spectra of a 4.5 μM solution of heme alone or in the presence of fragment 1−44 (10 μM) at a 1:2.25 molar ratio of heme/fragment. (B) UV−vis spectra of heme in the presence or absence of hGH and (C) with or without fragment 45−191. The concentration of hGH and fragment 45−191 was 5.1 μM and 1.9 μM, respectively. Both spectra B and C were recorded at a 1:1 molar ratio of heme:protein. Measurements were taken at room temperature in 20 mM Tris·HCl/0.15 M NaCl, pH 7.5.

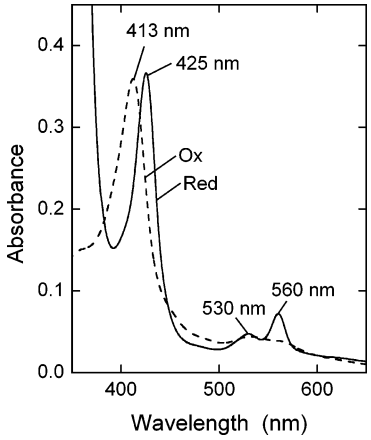

FIGURE 3: Absorption spectra of oxidized (− − −) and reduced (—) heme complex of fragment 1−44. UV−vis spectra of fragment 1−44 with oxidized and with reduced heme at a 0.6:1.0 molar ratio of heme:fragment (excess of fragment). Spectra were recorded in 20 mM Tris·HCl/0.15 M NaCl buffer, pH 7.5 at room temperature and a fragment concentration of 7.9 μM. Heme bound to fragment 1−44 was reduced by addition of a 1000-fold molar excess of sodium dithionite. The maxima in the two spectra are indicated.

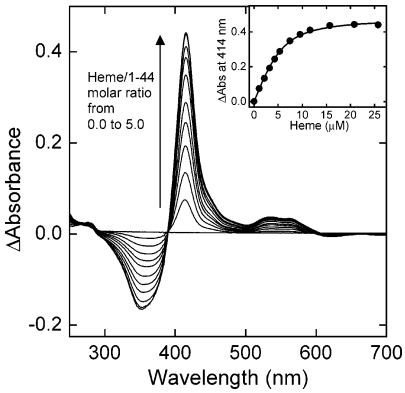

FIGURE 4: Titration of fragment 1−44 with heme. Difference absorption spectra acquired at increasing concentrations of heme over fragment 1−44. A hemin solution (0.58 mM in 0.1 M NaOH) was simultaneously added to a 5.3 μM solution of fragment 1−44 in 0.1 M Tris·HCl/0.15 M NaCl buffer, pH 7.5, and a reference cuvette containing Tris buffer only. After each addition of the heme solution, both the reference and the sample were stirred for 5 min and then allowed to stand for 5 min before spectra were acquired. The titration was performed at room temperature. The inset shows the heme-binding curve generated by plotting the difference absorbance at 414 nm versus the heme concentration.

conclusion was that fragment 1−44 and heme, despite their largely different molecular masses, eluted together from the gel filtration column, likely as a heme−fragment complex. The absorption spectrum of the complex eluted from the gel filtration column showed typical spectroscopic features of hemo-proteins (see below).

Absorption Spectra of Heme Bound to Fragment 1−44. The heme-binding capacity of fragment 1−44 was confirmed by adding a stock solution of Fe-protoporphyrin IX in 0.1 M NaOH to a solution of the fragment in Tris buffer, pH 7.5. The absorption spectrum of this solution was characterized by a Soret maximum at 413 nm and a broad band around 532 nm (Figure 2A). We investigated also the possibility that the complementary fragment 45−191 or hGH could bind the heme. To this aim, heme was added to solutions of these two protein species dissolved in Tris buffer, pH 7.5, under the same conditions used for fragment 1−44 and the absorption spectra of the solutions were recorded. As shown in Figure 2B,C, the features of the spectrum of heme do not change in the presence of added hGH or fragment 45−191, indicating the absence of a specific incorporation of heme into these protein species. Therefore, the property of heme binding is specific for fragment 1−44.

The absorption spectrum of heme bound to fragment 1−44 shows significant changes when reduced with sodium dithionite. As shown in Figure 3, the Soret band becomes slightly sharper and red-shifted to 425 nm, whereas in the α/β band region there is a pronounced splitting resulting in a well-resolved β-band at 530 nm and an α-band at 560 nm. These values are typical of bis-histidine ligated *b*-type cytochromes or of heme coordinated by one histidine and one methionine (*20*). Moreover, these spectral features are those of iron in a low-spin and hexacoordinated state (*24, 48*) (see also Discussion).

Heme−Fragment Dissociation Constant. The fact that fragment 1−44 retains a bound heme even after a gel filtration chromatographic step is a clear-cut indication of a strong affinity of heme for the fragment. Indeed, we measured the dissociation constant K_d between fragment 1−44 and heme, assuming that in solution heme does not exist in an aggregated state, but only in the free or bound state. A solution of fragment 1−44 at a fixed concentration was titrated with increasing amounts of heme, and difference absorption spectra were recorded against a solution of just buffer and heme. The increase in absorbance at 414 nm versus the heme concentration (Figure 4) was fitted to an equation for a 1:1 binding (*44*), and a figure of 1.48 μM ± 0.13 was calculated for the K_d of the complex.

Circular Dichroism Measurements. An interesting feature of the heme−fragment complex is that there is a change in the peptide secondary structure of fragment 1−44 upon heme binding. The far-UV CD spectra of the fragment with or without heme are shown in Figure 5. The spectrum of the complex has been acquired in the presence of an excess of heme (two equivalents), in order to shift the heme−fragment equilibrium toward the bound form. Whereas the CD

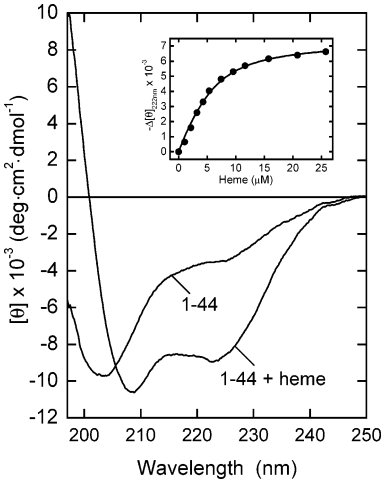

FIGURE 5: Far-UV CD spectra of fragment 1−44 in the absence and presence of heme. The molar ratio between fragment 1−44 and heme was 1:1.8 (excess of heme) at a fragment concentration of 5.3 μM. Spectra were recorded at 25 °C in 0.1 M Tris·HCl/0.15 M NaCl buffer, pH 7.5. The inset shows the titration curve obtained by plotting the $\Delta[\theta]_{222\text{ nm}}$ measured after each addition of heme to a solution of fragment 1−44 (5.3 μM) versus the heme concentration. The curve fitting was performed as described under Materials and Methods.

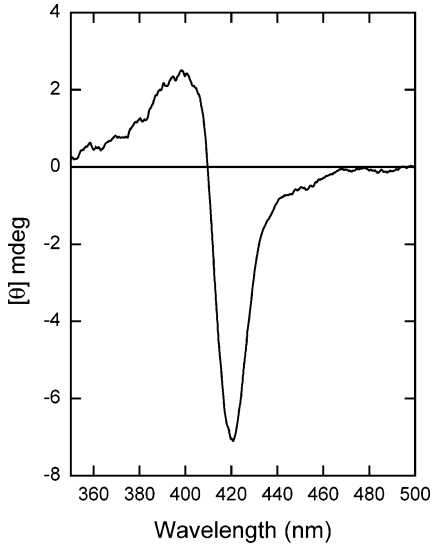

FIGURE 6: Induced CD spectrum in the Soret region of heme complexed with fragment 1−44. Spectra were recorded at 25 °C in 20 mM Tris·HCl/0.15 M NaCl buffer, pH 7.5. The concentration of heme was 38 μM, and the molar ratio of fragment:heme was 1:2 (excess of heme). The fragment concentration was 19.2 μM.

spectrum of fragment 1−44 in the absence of the Fe-protoporphyrin IX is that of a largely unfolded polypeptide, in the presence of heme the spectrum is characterized by minima of ellipticity at 208 and 222 nm, which are indicative of a significant degree of helicity (*49*). The far-UV CD spectra were analyzed in terms of percent helical secondary structure, and 9% and 26% helical content was calculated for free fragment and heme−fragment complex, respectively (*46*). However, it is known that estimates of percent helicity in polypeptides with a low content of secondary structure, as in the present case of fragment 1−44 alone, are not reliable (*49*). Moreover, the 26% of the heme−fragment complex can be in error, since the contribution of aromatic amino acid residues and chromophores to the far-UV CD spectra of polypeptides has been well documented, including that of the heme chromophore (*50, 51*). In particular, it has been concluded in these previous studies that the heme contribution to the far-UV CD spectrum of a heme-polypeptide leads to an underestimate of the actual helical content of the peptide/protein species.

The induction of secondary structure in fragment 1−44 upon heme binding was followed also by measuring the mean residue ellipticity at 222 nm at increasing concentrations of Fe-protoporphyrin IX. The data of ellipticity at 222 nm of the fragment versus the concentration of heme (Figure 5, inset) were fitted to the equation reported by Kuwabara et al. (*44*, see also ref *45*), and a K_d value of 2.33 μM ± 0.31 was estimated. This figure is quite similar to that obtained by absorption measurements (Figure 4). It may be that the slight difference can be attributed to the contribution of heme to far-UV CD ellipticities (see above), that can affect the estimate of K_d.

Symmetric chromophores that do not absorb circularly polarized light become optically active when they are embedded in a specific stereochemistry within a protein fold (*52*). This acquired optical activity is defined as induced circular dichroism (ICD), and it allows interesting protein−ligand binding studies (*53*). Heme does not have a signal in the visible region of the CD spectrum, if this moiety is free in solution or associated at the surface of a protein (*54*). However, upon binding to a protein in a chiral and relatively rigid environment, heme gives rise to characteristic ICD spectra. The optical activity of heme bound to fragment 1−44 was investigated in the Soret region (Figure 6). The CD spectrum is characterized by a maximum at 400 nm and a minimum at 420 nm, indicating that heme is bound to the fragment inside a relatively rigid pocket (*52*).

Resonance Raman Spectroscopy. In an attempt to possibly determine the amino acid side-chain residues of fragment 1−44 that act as ligands for the heme iron, resonance Raman (RR) measurements on the heme−fragment complex were carried out using an excitation wavelength in the Soret band at 413.1 nm (*47*). The high (ν_4, ν_3, ν_2, ν_{10} at 1373, 1504, 1576, and 1639 cm^{-1}, respectively) and low (ν_9 and ν_8 at 268 and 346 cm^{-1}) frequency region spectra of the complex showed frequencies typical of an Fe(III) in a hexacoordinated low spin state (not shown) (see ref *25*). However, a careful analysis of the RR spectra did not enable us to distinguish between a bis-His or a Met/His axial heme coordination (see Discussion).

Mass Spectrometry of the Heme−Fragment Complex. The stoichiometry of the binding between heme and fragment 1−44 was investigated also by electrospray ionization (ESI) mass spectrometry (MS). Indeed, recent advances of this technique and, in particular, the use of nano-electrospray allow one to analyze noncovalent protein complexes in solution at physiological pH and to measure their masses (*55*, *56*). Noncovalent interactions can be kept intact during the ionization process by carefully adjusting the parameters (mainly voltages and temperatures) of the mass spectrometer ion source.

For the ESI-MS analysis, we prepared a solution of heme and fragment 1−44 in 0.1 M ammonium acetate, pH 7.5, at a molar ratio of 2.0 (excess of heme) and we confirmed the formation of the complex under these solvent conditions by acquiring a UV−visible spectrum, which showed the typical

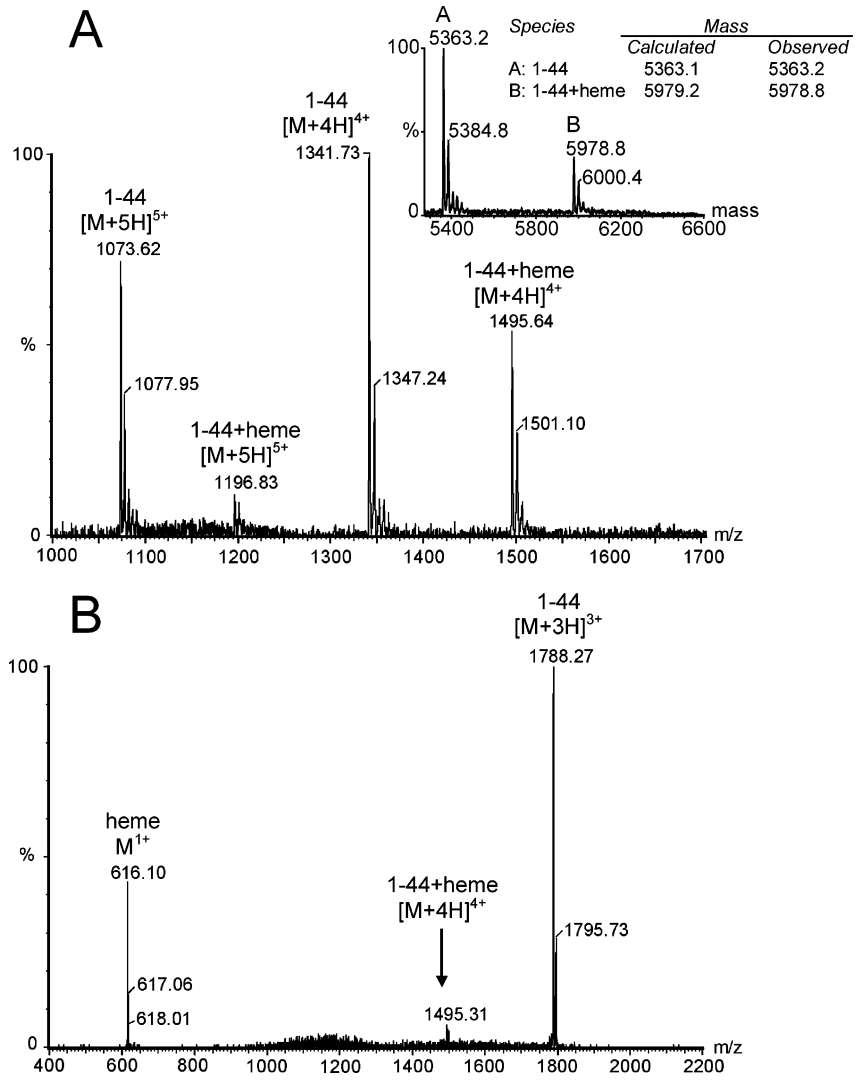

FIGURE 7: Mass spectrometric analysis of the heme−fragment 1−44 complex. (A) Electrospray mass spectrum of the heme−fragment complex. The identities and the charge states of each peak are indicated. The inset shows the deconvoluted mass spectra of (A) and the calculated and measured molecular masses of the various components. (B) MS/MS analysis of the charge state +4 of the heme−fragment complex. The identities and charge states of the dissociated species are indicated. The complex was analyzed in 0.1 M ammonium acetate buffer, pH 7.5, and the molar ratio heme:fragment was of 2:1 (excess of heme). The fragment concentration was 10 μM.

maxima of a hexacoordinated heme (see Figure 3 and Discussion). Analysis of this solution by nano-electrospray MS revealed the presence of multi-charge state peaks of fragment 1−44, together with a species of higher mass (Figure 7A). In particular, the measured mass of this last species, 5978.8 Da (Figure 7A, inset), corresponds to the calculated mass of the complex formed by fragment 1−44 (5363.1 Da) and heme (616.1 Da) at a 1:1 stoichiometry (calculated mass of the complex 5979.2 Da). In the mass spectrum there are no other species arising from a different stoichiometry of association between the fragment and the Fe-protoporphyrin IX. Moreover, we tested the ability of MS measurements to assess the specificity of heme binding by fragment 1−44. To this aim, we analyzed by MS a solution of hGH, fragment 45−191, and a tryptic digest of hGH in the presence of heme and we verified that heme binding does not occur (data not shown). On the other hand, MS and MS/MS analyses of a solution of apomyoglobin and heme gave clear-cut data of heme binding, as expected from the well-known binding of heme to apomyoglobin in a 1:1 molar ratio (*13*) (not shown).

In order to confirm the identity of the heme−fragment complex, we analyzed by MS/MS the charge state 4+ of the species of 5978.8 Da, which is the ion at 1495.64 *m*/*z* (see Figure 7A). Indeed, the MS/MS technique allows one to select an ion of interest and, in the case of a noncovalent complex, to dissociate it inside the mass spectrometer into its components and to measure their masses. The MS/MS spectrum thus acquired is shown in Figure 7B. It can be observed that the ion at 1495.64 *m*/*z* dissociates into a species at 616.1 *m*/*z*, which is the singly charged free ferric heme ion [Fe(III)heme]$^+$, and a species at 1788.27 *m*/*z*, that corresponds to the charge state +3 of fragment 1−44 without heme. Of interest, the ion +4 of the heme−fragment complex loses the positive charge associated to heme, thus leading to a triply protonated ion of the free fragment (*57*). Therefore, MS analysis confirmed the identity of the species of 5978.8 Da as the noncovalent complex between fragment 1−44 and heme at a 1:1 molar ratio.

Probing Fragment Structure by Proteolysis. We tested if a proteolytic probe could monitor the enhancement of secondary structure in fragment 1−44 upon heme binding,

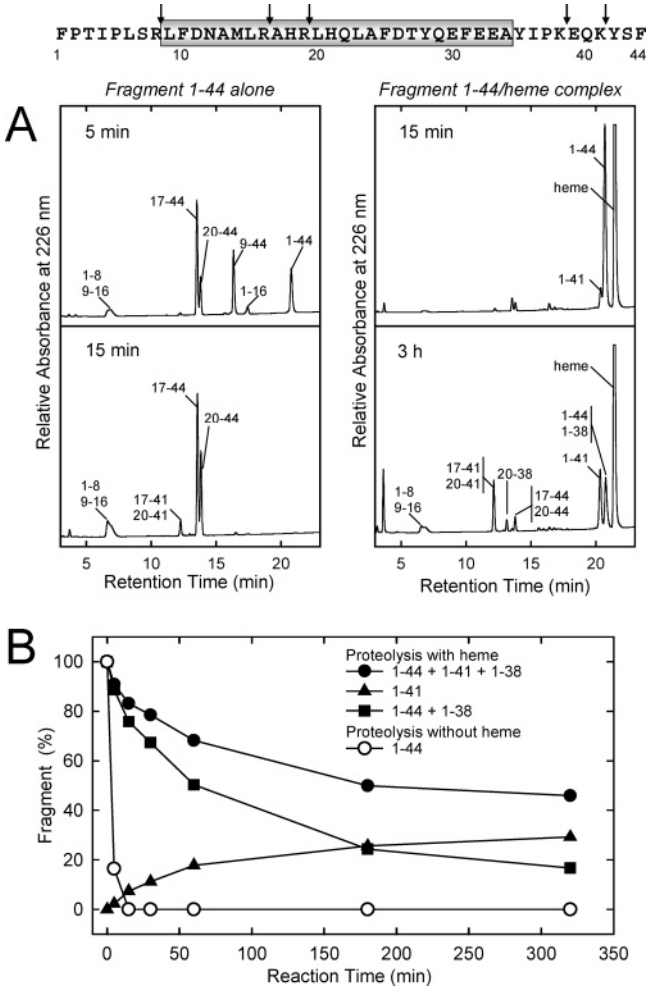

FIGURE 8: Limited proteolysis of fragment 1−44 in the absence or presence of heme with trypsin. (Top) Amino acid sequence of fragment 1−44. The location of the helix is indicated by a gray box (residues 9−34), whereas arrows indicate the sites of cleavage by trypsin. (A) RP-HPLC analysis of the proteolysis mixtures of fragment 1−44 with heme and without heme conducted at room temperature (E/S 1/500, by weight) in 20 mM Tris·HCl/0.15 M NaCl buffer, pH 7.5, at a molar ratio of 3:1 heme:fragment 1−44 (excess of heme). The fragment concentration was 0.07 mg/mL. Tryptic peptides separated by RP-HPLC were identified by ESI-MS. (B) The percent recovery of fragment 1−44 (in the absence of heme, open symbols)) and of fragments 1−44, 1−41, and 1−38 (in the presence of heme, closed symbols) during proteolysis reported vs the reaction time of the proteolysis reaction (see Materials and Methods).

as detected by far-UV CD measurements (see above Figure 5). Indeed, it is known that proteases easily attack unfolded or partly folded proteins, while folded native proteins are quite resistant to proteolysis (*8, 58*−*60*). Trypsin was chosen as a proteolytic probe, considering that the fragment contains up to five residues (Lys and Arg) which can be sites of tryptic attack, evenly distributed along its 44-residue chain (Figure 8, top). Solutions of fragment 1−44 alone or in the presence of heme at a 1:3 molar ratio of fragment:heme were digested in parallel with trypsin, and the time course of the digestion was determined by means of RP-HPLC analyses of aliquots taken at intervals from the reaction mixtures. The indentity of the various tryptic fragments was established by ESI-MS (Table 1). As shown in Figure 8A, the fragment alone is much more easily digested than the heme−fragment complex. Of interest, in the absence of heme, the tryptic peptides

Table 1: Molecular Masses of Tryptic Peptides of Fragment 1−44[a]

tryptic peptides of fragment 1−44	molecular mass (Da)	
	observed	calculated
1−44	5363.1	5363.1
1−41	4965.8	4965.7
1−38	4580.1	4580.2
9−44	4450.1	4451.0
17−44	3488.4	3487.7
20−44	3123.8	3123.5
17−41	3091.8	3090.5
20−41	2726.5	2726.3
20−38	2341.4	2341.1
1−16	1890.2	1890.0
9−16	978.6	978.5
1−8	929.6	929.5
42−44	415.2	415.2

[a] Tryptic peptides of fragment 1−44 were obtained by limited proteolysis of the fragment with trypsin at pH 7.5 in the presence or absence of heme, as described in the text. The mass spectrometric measurements were performed on the peptides isolated after RP-HPLC of the proteolytic mixtures. Experimental molecular masses were determined by ESI-MS, whereas theoretical average molecular masses were calculated from the amino acid sequence of fragment 1−44.

produced from fragment 1−44 derive from cleavages at all but one basic amino acid residue (Lys and Arg), since a tryptic peptide deriving from the hydrolysis of the Lys38−Glu39 peptide bond is not seen in the RP-HPLC chromatogram (Figure 8A). This derives from the fact that tryptic cleavages are hindered at basic residues flanked by acidic (Glu and Asp) residues (*61*). While the free fragment is fully digested by trypsin after 15 min reaction, in the presence of heme the fragment is almost fully resistant to proteolysis and only a small amount of fragment 1−41 is formed. Actually, MS analysis revealed that trace amounts of fragment 1−38 are also formed, this last fragment species being eluted together with the intact fragment from the RP-HPLC column. After 3 h reaction, other tryptic fragments are produced, but still fragment 1−44 remains quite abundant in the proteolysis mixture. Therefore, the proteolytic probe appears to trim the unstructured C-terminal end of the heme−fragment complex, in agreement with the fact that the heme−fragment complex adopts a hydrogen-bonded, helical secondary structure and that the first helix in intact hGH encompasses the chain segment 9−34 (*29*). Of note, the structural features of the N-terminal region of the fragment cannot be probed by trypsin, since with this specific protease peptide bond fission can occur only at Arg8 (see Figure 8, top). Upon prolonged proteolysis, such as 3 h reaction, the heme−fragment complex is slowly digested also at Arg16 and Arg19, both residues being located inside the helical chain segment 9−34. It is reasonable to propose that the equilibrium between the folded heme-bound fragment and the unfolded unbound species actually controls the proteolysis events, so that also the unfolded free fragment can act as tryptic substrate. The different rates of proteolysis of fragment 1−44 alone or in the presence of heme are better highlighted by calculating the percent decrease of intact fragment during proteolysis, as shown in Figure 8B. While fragment 1−44 alone is completely digested in few minutes, in the presence of heme the fragment is hydrolyzed much more slowly, concomitantly producing mostly fragment 1−41. If we consider the total percent of fragments 1−44, 1−41, and 1−38, we can observe that their combined amount

decreases only about 50% after 5 h of proteolysis of the fragment in the presence of heme (Figure 8, bottom).

DISCUSSION

In this paper, we report the novel observation that the hGH fragment 1−44 can bind the heme moiety. The binding property is not shared by fragment 45−191, nor by the entire hGH molecule. The spectrophotometric titration of fragment 1−44 with heme allowed us to deduce as 1:1 the molar ratio of the heme−fragment complex and a K_d of 1.48 μM. Additional evidence for both complex formation and stoichiometry was derived from ESI-MS measurements conducted on the complex at neutral pH. Clear-cut MS evidence of the 1:1 complex was obtained, since two main species were detected in the MS spectrum with a difference of their deconvoluted masses of 616 Da, corresponding to the mass of heme. Moreover, the MS/MS analysis of the complex resulted in the dissociation of the heme and concomitant appearance of the MS peaks of fragment and heme. No evidence for binding of two hemes to the fragment was obtained by MS measurements. The rather tight binding of heme to the fragment can be deduced, besides from the K_d value of the complex, from the fact that the complex can be separated by gel filtration chromatography. Moreover, the induced CD in the Soret region of the heme moiety, which is optically inactive in its free state in solution, is clearly indicative of a stereospecific binding of the heme in a quite rigid pocket of the folded fragment (*52*).

The interaction of heme with fragment 1−44 induces a significant amount of α-helical secondary structure in the otherwise largely unfolded fragment, as deduced from far-UV CD measurements. Assuming that the helix adopted by the fragment upon heme addition is similar to that of the corresponding chain region in the four-helix bundle hormone, the heme-mediated helix is expected to involve the chain segment 9−34 (helix A) (*29*) and to be strongly amphiphilic, as shown in Figure 9. It can be proposed that the hydrophobic face of the amphiphilic helix, made up mostly by Ala, Phe, and Leu residues, represents the docking site of the hydrophobic heme moiety (*11, 62*). As a matter of fact, in several studies it has been demonstrated that an amphiphilic helix is a key structural motif of synthetic polypeptides that are capable of heme binding (*20, 63*). A number of peptide models were constructed in such a way to form an amphiphilic helix that can bind heme. The hydrophilic and hydrophobic face of the helix contained mostly polar and charged (Glu, Lys) and hydrophobic (Phe, Leu) residues, respectively (see ref *20* for a review).

Limited proteolysis experiments conducted on the heme−fragment complex clearly demonstrated that the fragment adopts a quite rigid structure not amenable to an easy degradation by trypsin (*8, 58−60*). Proteolysis experiments were conducted using trypsin as proteolytic probe, considering that this substrate-specific enzyme can cleave at the C-terminus of Arg8, Arg16, Arg19, Lys38, and Lys41 (see Figure 8, top). Residues 16 and 19 are roughly in the middle of the first helix in native hGH (chain segment 9−34; *29*) and near the residues which can coordinate heme (Met14, His18, and His21). The folded, heme-bound fragment is rather resistant to proteolysis and is initially cleaved only at Lys41, while cleavage of the Lys38−Glu39 peptide bond is expected to be hindered by the presence of an acidic residue flanking the peptide bond to be hydrolyzed by trypsin (*61*). Therefore, considering that Arg8 is at or near the N-terminus of helix 9−34 of intact hGH, limited proteolysis of the folded fragment occurs in agreement with the boundaries of the expected helix. On the opposite, proteolysis of the fragment alone is very fast and leads to the preferential hydrolysis at the level of residues 8, 16, and 19, indicating that the helix is not present.

The heme binding to the fragment likely involves, besides a simple docking of heme to the hydrophobic face of the amphiphilic helix of the fragment, also some specific ligands that make the complex stronger and more specific. The UV−visible absorption spectra of the complex show characteristics of a hexacoordinated heme iron (see Results). Fragment 1−44 contains His18, His21, and Met14 (Figure 9), i.e., amino acid residues whose side chains are known to be favored ligands in cytochromes (*64*). Both bis-His and Met/His ligations occur in cytochromes, with His/His coordination predominating both in the *b*-type and in *c*-type cytochromes. The Met/His heme iron ligation occurs in the covalently attached heme of horse cytochrome *c* (*65*), as well as in the noncovalently bound heme of the four-helix bundle protein cytchrome b_{562} (*66*) and in the fungal flavocytochrome cellobiose dehydrogenase (*67*). Therefore, it can be proposed that a bis-His or a Met/His complex is formed by fragment 1−44 using two His or one His and Met14, respectively, as ligands. Unfortunately, the UV−visible absorption spectra of oxidized and reduced heme bound to fragment 1−44 cannot be used to distinguish whether a bis-His or Met/His complex is formed, since the two types of complexes have similar maxima in their UV−visible absorption spectra (*20, 68*). The weak absorption band at 695 nm, often regarded as diagnostic for the methionine ligation to the heme iron, was not observed with the heme−fragment complex. However, the absence of this band does not necessarily indicate that a methionine ligand is missing (see *69*). Perhaps, even the Tyr residues of the fragment 1−44 (Tyr28, Tyr35, and Tyr42) can play a role in heme binding, since Tyr is weakly nucleophilic and it acts as a heme ligand in *Serratia* hemophore and in few other proteins (see ref *70* for references). However, the very easy and fast proteolytic cleavage of the C-terminal portion of the heme−fragment complex seems to exclude at least Tyr42 as a heme ligand (see Figure 8).

Resonance Raman (RR) measurements were conducted on the heme−fragment complex, hoping to possibly determine the amino acid side chains of fragment 1−44 which coordinate heme. The characteristics of the RR spectra were consistent with an Fe(III) in a hexacoordinate low spin state, but the spectra did not enable us to distinguish between a bis-His or a Met/His axial heme coordination (data not shown). Perhaps, NMR studies could be conducted in order to identify the heme coordinating residues, but the low solubility of fragment 1−44 does not allow one to reach the fragment concentration required for NMR measurements. Therefore, additional studies are required in order to firmly ascertain the ligands in the heme−fragment complex.

It is not known yet if heme binding to hGH fragment 1−44 does occur in vivo and thus if this binding has a physiological significance. Heme in vivo is produced in the plasma upon rupture of the blood cells, as a result of hemolysis, trauma,

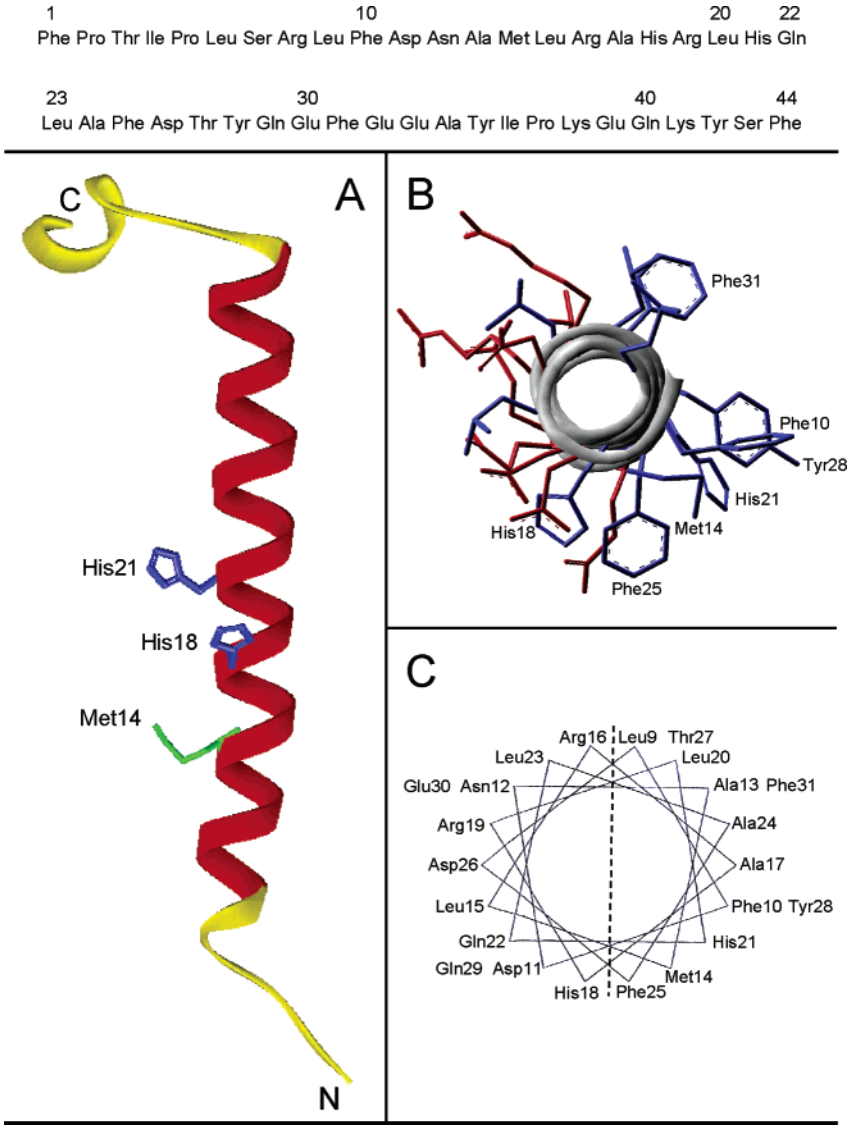

FIGURE 9: Structural features of fragment 1−44. (Top) Amino acid sequence of fragment 1−44. (Bottom) Three-dimensional structure (A) of fragment 1−44 of hGH derived from the X-ray structure of the protein (Brookhaven Protein Data Bank 3HHR) using the program WebLab Viewer Pro 4.0 (Molecular Simulations Inc., San Diego, CA). The first helix of hGH (residues 9−34) is colored in red, and amino acid residues relevant to the discussion of the results of this study are colored in blue (His) and green (Met). (B) The region 9−31 of helix 9−34 is shown looking through the helix axis. Hydrophobic and hydrophilic residues are colored in blue and in red, respectively, in order to illustrate the amphiphilicity of the helix. (C) The same region 9−31 of the helix is also represented in a helix wheel drawing, and the hydrophobic side of the helix is separated from the hydrophilic one by a dashed line.

and ischemia. It is currently accepted that free heme does not exist in vivo, since it has toxic effects, but that it is strongly bound to hemopexin and albumin. Hemopexin is the strongest heme-binding protein in plasma (K_b 10^9 M^{-1}) (*10*), but its abundance is low (10−20 μM) and, therefore, a protective effect from heme can be exerted by other heme-binding proteins. It has been proposed that the most abundant protein albumin can serve as a heme-carrier, when hemopexin is saturated (*71*). At present, we can speculate that, if heme binding occurs, the hGH fragment adopts a folded structure that makes it rather resistant to proteolytic degradation. The properties of fragment 1−44, produced in vitro by proteolysis of the hormone (*39*), are expected to be very similar to those of fragment 1−43, which is circulating in vivo and shows hypoglycemic activity (*33*, *34*, *38*). If we accept this, it is quite unlikely that the naturally occurring fragment 1−43 circulates in vivo as a largely unfolded chain, since it can be anticipated that this random polypeptide would be degraded rapidly by proteases. Therefore, a stabilization of this largely unfolded fragment by a mechanism of binding and folding is necessary, as earlier proposed for intrinsically unstructured or "natively unfolded" proteins (*72*).

Summing up, the interest of this study resides in the fact that heme-binding is observed with a polypeptide species that appears to be physiologically relevant. The hGH fragment 1−44 can be an interesting model for further studies of the molecular mechanisms of heme binding to polypeptides. Indeed, nowadays numerous investigators are involved in studying a variety of model systems in an attempt to provide insights into structure−function relationships of heme−protein interactions and reproduce in relatively small polypeptides the biological properties of the natural heme-proteins that in vivo catalyze some vital bioenergetic reactions (*17*, *20*, *28*, *73*). Finally, we may add here that perhaps the observation that a largely unfolded polypeptide chain can bind heme and that binding results in the induction

and stabilization of peptide structure can have biomedical implications, as follows. It has been found that partly folded and "natively unfolded" proteins can be intermediates in the protein aggregation processes that cause severe neurodegenerative diseases (Parkinson, Alzheimer) (*74*, *75*). Heme binding can occur with unstructured proteins, preventing protein aggregation and ultimately the formation of amyloid deposits (*76*−*79*). Therefore, the ability of heme to induce and stabilize protein structure can be a mechanism involved in the inhibition of protein aggregation.

ACKNOWLEDGMENT

We thank Dr. Patrizia Polverino de Laureto for insightful comments on this paper and Marcello Zambonin for excellent technical assistance. We acknowledge Prof. Angela Lombardi and Prof. Giulietta Smulevich for important suggestions and Dr. Barry D. Howes for performing resonance Raman spectroscopy measurements.

REFERENCES

1. Dolphin, D., Ed. (1979) *The Porphyrins*, Vol. 7, Academic Press, New York.
2. Padmanaban, G., Venkateswar, V., and Rangarajan, P. N. (1989) Heme as a multifunctional regulator, *Trends Biochem. Sci. 14*, 492−496.
3. Feng, Y., Sligar, S. G., and Wand, A. J. (1994) Solution structure of apocytochrome b_{562}, *Nat. Struct. Biol. 1*, 30−35.
4. Falzone, C. J., Mayer, M. R., Whiteman, E. L., Moore, C. D., and Lecomte, J. T. (1996) Design challenges for hemoproteins: The solution structure of apocytochrome b_5, *Biochemistry 35*, 6519−6526.
5. Eliezer, D., and Wright, P. E. (1996) Is apomyoglobin a molten globule? Structural characterization by NMR, *J. Mol. Biol. 263*, 531−538.
6. Robinson, C. R., Liu, Y., Thomson, J. A., Sturtevant, J. M., and Sligar, S. G. (1997) Energetics of heme binding to native and denatured states of cytochrome b_{562}, *Biochemistry 36*, 16142−16146.
7. Dumont, M. E., Corin, A. F., and Campbell, G. A. (1994) Noncovalent binding of heme induces a compact apocytochrome *c* structure, *Biochemistry 33*, 7368−7378.
8. Spolaore, B., Bermejo, R., Zambonin, M., and Fontana, A. (2001) Protein interactions leading to conformational changes monitored by limited proteolysis: Apo form and fragments of horse cytochrome *c*, *Biochemistry 40*, 9460−9468.
9. Baltzer, L. (1998) Functionalization of designed folded polypeptides, *Curr. Opin. Struct. Biol. 8*, 466−470.
10. Hrkal, Z., Vodrazka, Z., and Kalousek, I. (1974) Transfer of heme from ferrihemoglobin and ferrihemoglobin isolated chains to hemopexin, *Eur. J. Biochem. 43*, 73−78.
11. Leclerc, E., Leclerc, L., Poyart, C., and Marden, M. C. (1993) Interaction of heme with amphiphilic peptides: Use of hemin-CN to probe the interaction of calmodulin with its target peptides, *Arch. Biochem. Biophys. 306*, 158−162.
12. Marden, M. C., Dufour, E., Christova, P., Huang, Y., Leclerc, E., and Haertlé, T. (1994) Binding of heme-CO to bovine and porcine β-lactoglobulin, *Arch. Biochem. Biophys. 311*, 258−262.
13. Hargrove, M. S., Barrick, D., and Olson, J. S. (1996) The association rate constant for heme binding to globin is independent of protein structure, *Biochemistry 35*, 11293−11299.
14. Zhang, L., and Guarente, L. (1995) Heme binds to a short sequence that serves a regulatory function in diverse proteins, *EMBO J. 14*, 313−320.
15. Wardell, M., Wang, Z., Ho, J. X., Robert, J., Ruker, F., Ruble, J., and Carter, D. C. (2002) The atomic structure of human Methemalbumin at 1.9 Å, *Biochem. Biophys. Res. Commun. 291*, 813−819.
16. Poulos, T. (1995) The role of proximal ligand in heme enzymes, *J. Bioinorg. Chem. 1*, 356−359.
17. Reedy, C. J., and Gibney, B. R. (2004) Heme protein assemblies, *Chem. Rev. 104*, 617−649.
18. Nastri, F., Lombardi, A., D'Andrea, L. D., Sanseverino, M., Maglio, O., and Pavone, V. (1998) Miniaturized hemoproteins, *Biopolymers 47*, 5−22.
19. Rau, H. K., and Haehnel, W. (1998) Design, synthesis and properties of a novel cytochrome *b* model, *J. Am. Chem. Soc. 120*, 468−476.
20. Lombardi, A., Nastri, F., and Pavone, V. (2001) Peptide-based heme-protein models, *Chem. Rev. 101*, 3165−3189.
21. Gibney, B. R., and Dutton, P. L. (2000) *De novo* design and synthesis of heme proteins, in *Advances in Inorganic Chemistry* (Mauk, A. G., and Sykes, A. G., Eds.) Vol. 51, pp 409−455, Academic Press, London.
22. Hecht, M. H., Richardson, J. S., Richardson, D. C., and Ogden, R. C. (1990) *De novo* design, expression and characterization of Felix: A four-helix bundle protein of native-like sequence, *Science* 249, 884−891.
23. Robertson, D. E., Farld, R. S., Moser, C. C., Urbauer, J. L., Mulholland, S. E., Pidikiti, R., Lear, J. D., Wand, A. J., De Grado, W. F. and Dutton, P. L. (1994) Design and synthesis of multi-heme proteins, *Nature 368*, 425−432.
24. Choma, C. T., Lear, J. D., Nelson, M. J., Dutton, P. L., Robertson, D. E., and De Grado, W. F. (1994) Design of a heme-binding four-helix bundle, *J. Am. Chem. Soc. 116*, 856−865.
25. Rojas, N. R. L., Kamtekar, S., Simone, C. T., Mc Lean, J. E., Vogel, K. H., Spiro, T. G., Farid, R. S., and Hecht, M. H. (1997) *De novo* heme proteins from designed combinatorial libraries, *Protein Sci. 6*, 2512−2524.
26. Gibney, B. R., Rabanal, F., Reddy, K. S., and Dutton, P. L. (1998) Effect of four-helix bundle topology on heme binding and redox properties, *Biochemistry 37*, 4635−4643.
27. De Grado, W. F., Summa, C. M., Pavone, V., Nastri, F., and Lombardi, A. (1999) *De novo* design and structural characterization of proteins and metalloproteins, *Annu. Rev. Biochem. 68*, 779−819.
28. Ghirlanda, G., Osyczka, A., Liu, W., Antolovich, M., Smith, K. M., Dutton, P. L., Wand, A. J., and De Grado, W. F. (2004) *De novo* design of a D2-symmetrical protein that reproduces the diheme four-helix bundle in cytochrome *cb*1, *J. Am. Chem. Soc. 126*, 8141−8147.
29. de Vos, A. M., Ultsch, M., and Kossiakoff, A. A. (1992) Human growth hormone and extracellular domain of its receptor: Crystal structure of the complex, *Science 255*, 306−312.
30. Li, C. H. (1982) Human growth hormone: 1974−1981, *Mol. Cell. Biochem. 46*, 31−41.
31. Silva, C. M., Isgaard, J., and Thorner, M. O. (1998) Cytokines in endocrine function, *Adv. Protein Chem. 52*, 199−221.
32. Okada, S., and Kopchick, J. J. (2001) Biological effects of growth hormone and its antagonist, *Trends Mol. Med. 7*, 126−132.
33. Lewis, U. J., Sinha, Y. N., and Lewis, G. P. (2000) Structure and properties of members of the hGH family: A review, *Endocr. J. 47*, Suppl., S1−S8.
34. Singh, R. N. P., Seavey, B. K., Lewis, L. J., and Lewis, U. J. (1983) Human growth hormone peptide 1−43: Isolation from pituitary glands, *J. Protein Chem. 2*, 425−436.
35. Frigeri, L. G., Teguh, C., Ling, N., Wolff, G. L., and Lewis, U. J. (1988) Increased sensitivity of adipose tissue to insulin after in vivo treatment of yellow Avy/A obese mice with amino-terminal peptides of human growth hormone, *Endocrinology 122*, 2940−2945.
36. Lewis, U. J., Lewis, L. J., Salem, M. A., Staten, N. R., Galosy, S. S., and Krivi, G. G. (1991) A recombinant-DNA-derived modification of human growth hormone (hGH44−191) with enhanced diabetogenic activity, *Mol. Cell. Endocrinol. 78*, 45−54.
37. Sinha, Y. N., and Jacobsen, B. P. (1994) Human growth hormone (hGH)-(44−191), a reportedly diabetogenic fragment of hGH, circulates in human blood: Measurement by radioimmunoassay, *J. Clin. Endocrinol. Metab. 78*, 1411−1418.
38. Lopez-Guajardo, C. C., Armstrong, L. S., Jordan, L., Staten, N. R., Krivi, G. G., Martinez, A. O., and Haro, L. S. (1998) Generation, characterization and utilization of anti-human growth hormone 1−43 (hGH1−43), monoclonal antibodies in an ELISA, *J. Immunol. Methods 215*, 179−185.
39. Spolaore, B., Polverino de Laureto, P., Zambonin, M., and Fontana, A. (2004) Limited proteolysis of human growth hormone at low pH: Isolation, characterization and complementation of the two biologically relevant fragments 1−44 and 45−191, *Biochemistry 43*, 6576−6586.
40. Franchi, E, Maisano, F., Testori, S. A., Galli, G., Toma, S., Parente, L., de Ferra, F., and Grandi, G. (1991) A new human growth

hormone production process using a recombinant *Bacillus subtilis* strain, *J. Biotechnol. 18*, 41−54.
41. Gill, S. C., and von Hippel, P. H. (1989) Calculation of protein extinction coefficients from amino acid sequence data, *Anal. Biochem. 182*, 319−326.
42. Dawson, R. M. C., Elliott, D. C., Elliott, W. H., and Jones, K. M. (1975) *Data for Biochemical Research*, pp 230−231, Oxford University Press, Oxford, U.K.
43. Tsutsui, K., and Mueller, G. C. (1982) A protein with multiple heme-binding sites from rabbit serum, *J. Biol. Chem. 257*, 3925−3931.
44. Kuwabara, T., Nakamura, A., Ueno, A., and Toda, F. (1994) Inclusion complexes and guest-induced color changes of pH-indicator-modified β-cyclodextrins, *J. Phys. Chem. 98*, 6297−6303.
45. Sakamoto, S., Sakurai, S., Ueno, A., and Mihara, H. (1997) Heme binding and catalytic activity of two-α-helix peptide annealed by trifluoroethanol, *Chem. Commun. 13*, 1221−1222.
46. Scholtz, J. M., Qian, H., York, E. J., Stewart, J. M., and Baldwin, R. L. (1991) Parameters of helix-coil transition theory for alanine-based peptides of varying chain lengths in water, *Biopolymers 31*, 1463−1470.
47. Santoni, E., Scatragli, S., Sinibaldi, F., Fiorucci, L., Santucci, R., and Smulevich, G. (2004) A model for the misfolded bis-His intermediate of cytochrome *c*: The 1-56 N-fragment, *J. Inorg. Biochem. 98*, 1067−1077.
48. Babcock, G. T., Widger, W. R., Cramer, W. A., Oertling, W. A., and Metz, J. G. (1985) Axial ligands of chloroplast cytochrome *b*-559: Identification and requirement for a heme-crosslinked polypeptide structure, *Biochemistry 24*, 3638−3645.
49. Kelly, S. M., Jess, T. J., and Price, N. C. (2005) How to study proteins by circular dichroism, *Biochim. Biophys. Acta 1751*, 119−139.
50. Benson, D. R., Hart, B. R., Zhu, X., and Doughty, M. B. (1995) Design, synthesis, and circular dichroism investigation of peptide-sandwiched mesoheme, *J. Am. Chem. Soc. 117*, 8502−8510.
51. Nicola, N. A., Minasian, E., Appleby, C. A., and Leach, S. J. (1975) Circular dichroism studies of myoglobin and leghemoglobin, *Biochemistry 14*, 5141−5149.
52. Myer, Y. P. (1978) Circular dichroism spectroscopy of emoproteins, *Methods Enzymol. 54*, 249−284.
53. Dockal, M., Carter, D. C., and Ruker, F. (1999) The three recombinant domains of human serum albumin: Structural characterization and ligand binding properties, *J. Biol. Chem. 274*, 29303−29310.
54. Ihara, M., Takahashi, S., Ishimori, K., and Morishima, I. (2000) Functions of fluctuation in the heme-binding loops of cytochrome b_5 revealed in the process of heme incorporation, *Biochemistry 39*, 5961−5970.
55. Hernandez, H., and Robinson, C. V. (2001) Dynamic protein complexes: Insights from mass spectrometry, *J. Biol. Chem. 276*, 46685−46688.
56. Sobott, F., and Robinson, C. V. (2002) Protein complexes gain momentum, *Curr. Opin. Struct. Biol. 12*, 729−734.
57. He, F., Hendrickson, C. L., and Marshall, A. G. (2000) Unequivocal determination of metal atom oxidation state in naked heme proteins: Fe(III)myoglobin, Fe(III)cytochrome *c*, Fe(III)cytochrome *b*5, and Fe(III)cytochrome *b*5 L47R, *J. Am. Soc. Mass Spectrom. 11*, 120−126.
58. Fontana, A., Fassina, G., Vita, C., Dalzoppo, D., Zamai, M., and Zambonin, M. (1986) Correlation between sites of limited proteolysis and segmental mobility in thermolysin, *Biochemistry 25*, 1847−1851.
59. Fontana, A., Zambonin, M., Polverino de Laureto, P., De Filippis, V., Clementi, A., and Scaramella, E. (1997) Probing the conformational state of apomyoglobin by limited proteolysis, *J. Mol. Biol. 266*, 223−230.
60. Fontana, A., Polverino de Laureto, P., Spolaore, B., Frare, E., Picotti, P., and Zambonin, M. (2004) Probing protein structure by limited proteolysis, *Acta Biochim. Pol. 51*, 299−321.
61. Ambler, R. P., and Brown, L. H. (1967) The amino acid sequence of *Pseudomonas* fluorescent azurin, *Biochem. J. 104*, 784−825.
62. Huffman, D. L., and Suslik, K. S. (2000) Hydrophobic interactions in metalloporphyrin-peptide complexes, *Inorg. Chem. 39*, 5418−5419.
63. Huffman, D. L., Rosenblatt, M. M., and Suslick, K. S. (1998) Synthetic heme-peptide complexes, *J. Am. Chem. Soc. 120*, 6183−6184.
64. Moore, G. R., and Pettigrew, G. W. (1990) *Cytochromes c: Evolutionary, Structural and Physicochemical Aspects*, Springer-Verlag, New York.
65. Bushnell, G. W., Louie, G. V., and Brayer, G. D. (1990) High-resolution three-dimensional structure of horse heart cytochrome *c*, *J. Mol. Biol. 214*, 585−595.
66. Hay, S., and Wydrzynski, T. (2005) Conversion of the *Escherichia coli* cytochrome *b*562 to an archetype cytochrome *b*: A mutant with bis-histidine ligation of heme iron, *Biochemistry 44*, 431−439.
67. Rotsaert, F. A., Hallberg, B. M., de Vries, S., Moenne-Loccoz, P., Divne, C., Renganathan, V., and Gold, M. H. (2003) Biophysical and structural analysis of a novel heme B iron ligation in the flavocytochrome cellobiose dehydrogenase, *J. Biol. Chem. 278*, 33224−33231.
68. Ishida, M., Dohmae, N., Shiro, Y., Oku, T., Iizuka, T., and Isogai, Y. (2004) Design and synthesis of *de novo* cytochromes *c*, *Biochemistry 43*, 9823−9833.
69. Rosell, F. I., and Mauk, A. G. (2002) Spectroscopic properties of a mitochondrial cytochrome *c* with a single thioether bond to the heme prosthetic group, *Biochemistry 41*, 7811−7818.
70. Deniau, C., Gilli, R., Izadi-Pruneyre, N., Letoffe, S., Delepierre, M., Wandersman, C., Briand, C., and Lecroisey, A. (2003) Thermodynamics of heme binding to the HasA(SM) hemophore: Effect of mutations at three key residues for heme uptake, *Biochemistry 42*, 10627−10633.
71. Peters, T., Jr. (1996) *All about Albumins: Biochemistry, Genetics and Medical Applications*, Academic Press, San Diego, CA.
72. Wright, P. E., and Dyson, H. J. (1999) Intrinsically unstructured proteins: Re-assessing the protein structure-function paradigm, *J. Mol. Biol. 293*, 321−331.
73. Rosenblatt, M. M., Wang, J., and Suslick, K. S. (2003) *De novo* designed cyclic-peptide heme complexes, *Proc. Natl. Acad. Sci. U.S.A. 100*, 13140−13145.
74. Dobson, C. M. (2003) Protein folding and disease: A view from the first Horizon Symposium, *Nat. Rev. Drug Discov. 2*, 154−160.
75. Uversky, V. N., and Fink, A. L. (2004) Conformational constraints for the amyloid fibrillation: The importance of being unfolded, *Biochim. Biophys. Acta 1698*, 131−153.
76. Howlett, D., Cutler, P., Heales, S., and Camilleri, P. (1997) Hemin and related porphyrins inhibit beta-amyloid aggregation, *FEBS Lett. 417*, 249−251.
77. Caughey, W. S., Raymond, L. D., Horiuchi, M., and Caughey, B. (1998) Inhibition of protease-resistant prion protein formation by porphyrins and phthalocyanines, *Proc. Natl. Acad. Sci. U.S.A. 95*, 12117−12122.
78. Priola, S. A., Raines, A., and Caughey, W. S. (2000) Porphyrin and phthalocyanine antiscrapie compounds, *Science 287*, 1503−1506.
79. Pato, C., Celier, C., Rezael, H., Grosclaude, J., and Marden, M. C. (2004) Heme as an optical probe of conformational transition of ovine recPrP, *Protein Sci. 13*, 1100−1107.

BI051374D